Thermographic Quantification for Archaeological Prospection at Picuris Pueblo, New Mexico

Samuel Levin
Geospatial Information Sciences
The University of Texas at Dallas
Richardson, Texas, United States
samuel.levin@utdallas.edu

May Yuan
Geospatial Information Sciences
The University of Texas at Dallas
Richardson, Texas, United States
myuan@utdallas.edu

Michael Adler
Anthropology
Southern Methodist University
Dallas, Texas, United States
madler@smu.edu

***Abstract*—This paper contributes to advancing thermal remote sensing for archaeological research. It proposes a new quantitative analysis of thermal imagery for subsurface feature prospection. Modern research trends and existing thermal remote sensing methods in archaeology are examined. Expanding on these methods, this study explores a new thermal imagery processing workflow with spatiotemporal variables extracted from a time series of thermal orthophotos. This proposed thermographic quantification enhances the thermal signature of subtle subsurface features on site, allowing undocumented structural features to be identified. This workflow is applied in a case study at Picuris Pueblo, New Mexico. Multi-temporal thermal signatures are processed using an original image differencing method. Using known subsurface features as training data, the thermal signatures of uninvestigated areas are classified to identify probable subsurface architectural features. The case study demonstrates the efficacy of the proposed thermal imagery processing method for subsurface feature detection and archaeological prospection. This method provides a non-destructive approach to studying Picuris Pueblo and similar occupation sites across archaeological landscapes, allowing contemporary research questions to be addressed.**

Keywords— Thermography, Archaeology, Remote Sensing, Drone, Image Processing

I. Introduction

Few fields have embraced the immense potential of geospatial information (GI) technologies to the extent of archaeology. Indeed, the accessibility of modern geospatial information science and technology has been touted as one of the most significant assets for archaeologists since the advent of carbon-14 dating. Now ubiquitous in the modern archeologist's tool kit, GI technologies are used for everything from cataloging site data to analysis of complex trade networks. Yet perhaps the most explosive growth of geospatial applications in archaeology has been in remote sensing. Enabling vastly increased survey breadth and meticulous documentation of sites, the relatively recent accessibility of remote sensing technologies has revolutionized the way archaeological research is conducted.

Among the many goals of archaeological research, remote sensing has a unique capacity to contribute to site prospection objectives. Site prospection (or site detection) can be understood as the identification of new or previously unknown sites or archaeological features. This can occur in areas with previously documented surrounding archaeological activities, or likewise in new areas without proximal site locations.

Aerial thermography is an emerging subset of remote sensing research with significant potential in this arena. This study seeks to assess the existing state of thermographic remote sensing for archaeological prospection by identifying its most common applications and the methods that enable them. Expanding on the existing research, this study proposes a new thermographic quantification (TQ) approach to enhance the archaeological efficacy of thermal remote sensing for subsurface archaeological features prospection, in this case the presence of adobe architectural features.

The methods developed here are applied in a pilot study at Picuris Pueblo, New Mexico. Picuris Pueblo is a Northern Tiwa-speaking Native American community in northern New Mexico (Fig. 1). The proposed TQ approach is used to infer the presence of subsurface architectural features in the areas surrounding the above-ground pueblo remains. Identification and future investigation of these features help elucidate pressing research questions, including delineation of the pueblo's maximum extent.

II. Aerial Thermography for Site Prospection

Once a cost prohibitive method, thermal remote sensing, or thermography, has experienced an uptick in popularity in recent years. This rising popularity has largely been driven by the diminishing price of thermal sensors from companies such as FLIR and accessibility of Small Unmanned Aircraft Systems (sUAS). A sUAS platform can capture imagery with greater

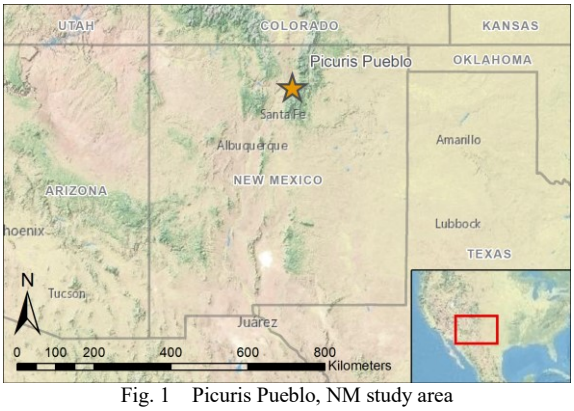

Fig. 1 Picuris Pueblo, NM study area

978-1-7281-0292-4/18/$31.00 ©2018 IEEE

spatial and temporal resolution, far beyond what is possible from satellite thermal imagery. Thermal remote sensing has unique potential to contribute to archaeological site prospection as a method for inferring the presence of subsurface architectural features. Of course, this ability is of particular interest to archaeology where the data potential of buried materials often exceeds that of materials on the surface.

Thermographic applications in archaeology depend on the basic principles of thermal remote sensing. All matter with a temperature above absolute zero emits radiant flux, which can be measured by a sensor to infer the radiant temperature of the material. However, there is not a perfect relationship between radiant temperature and true kinetic temperature. Due to emissivity, the radiant temperature of an object is always less than its true kinetic temperature. The lower the emissivity of a material, the greater the disparity between radiant and true temperature [1]. Thus, materials with the same kinetic temperature can have different radiant temperatures if their emissivity is sufficiently different.

Detection of subsurface features requires the effects of thermal inertia to be incorporated. Thermal inertia describes the relationship of thermal conductivity and volumetric heat capacity, which influences the thermal response of a material to surrounding temperature changes. The higher a material's thermal inertia, the more it resists changes in temperature. Conversely, a material with lower thermal inertia changes temperature more readily than one with higher thermal inertia. Thus, a subsurface material of different thermal inertia from its surrounding soil matrix will retain or lose heat at a different rate. If this contrast is sufficient, it can affect the temperature of the surrounding soils, producing differences in surface radiance detectable by the sensor [2]. Harnessing these thermal properties is critical to successful thermographic prospection of archaeological contexts.

Perhaps the most significant factor driving thermal remote sensing in archaeology is the rapidly expanding capabilities of Small Unmanned Aircraft Systems (sUAS). Deceases in the costs of these platforms have vastly increased the accessibility of project-specific remote sensing and data acquisition. Hobbyists drones, miniaturized sensors, and automated flight controllers are enabling archaeologists to rapidly deploy remote sensing technologies on sites. Moreover, these platforms can follow customized data collection strategies to meet project's multi-resolution requirements. Indeed, the highly adaptable nature of drone platforms enables data collections at spatial, temporal, and spectral resolutions tailored to project's objectives and has been critical to the success of numerous investigations [3]. Presently there are few publications that involve in the use of drone-based thermal remote sensing in archaeology, largely due to the relatively recent accessibility of such technologies.

In a recent application of thermography to archaeological prospection, researchers conducted a thermal remote sensing survey of the Chaco-era Blue J community in New Mexico. Using a drone based FLIR sensor, the study area was surveyed four times over the course of a day. By visually comparing the thermograms to reflective imagery of the study area, several thermal anomalies were identified, seeming to indicate unexcavated, subsurface architectural remains. These features were most visible in the early morning thermogram and were inferred to be stone walls. These walls appeared as warm anomalies due to their high thermal inertia relative to the surrounding soil matrix, retaining heat through the night while the surrounding area cooled down more rapidly. Perhaps most exciting, this investigations identified subsurface features in conditions ill-suited to geophysical methods such as magnetic gradiometry. In this rough, rocky environment, it appeared that aerial thermography had a decisive edge over conventional geophysical methods [4].

In a later report detailing the results of several similar case studies, the importance of survey timing in thermographic research was emphasized. Since thermal inertia induced contrast between subsurface materials and their surrounding soils varies throughout the day, these differences may only be visible during certain temporal windows. Thus, multiple flights throughout the day are recommended in hopes of capturing these differences when most pronounced. Experiments with some limited image processing methods were also explored, including NDVI transformations to correct the masking effects of vegetation on thermal imagery [5]. This work underscored the profound effect of environmental conditions on the effectiveness of thermography, noting that various conditions can produce unpredictable results. Conditions such as soil moisture, ground cover, and diurnal temperature range all affect the ability of the sensor to produce meaningful images.

In an experimental investigation, researchers designed a test plot of simulated buried archaeological features to test the effectiveness of aerial thermography at resolving each feature in varied environmental conditions. Twenty-six thermograms of the plot were generated over a period of two months, capturing the varied effects of precipitation, ambient temperature, and other factors on the features. From these images, visual analysis was used to identify anomalous thermal signatures indicative of the subsurface test features. This investigation also experimented with a limited number of quantitative image processing methods, including calculation of the mean and standard deviation from a series of thermograms. While the standard deviation image produced no significant information, the mean image enhanced some buried features relative to individual thermograms. Another experiment attempted to remove vegetation-induced noise from thermal imagery by subtracting the Normalized Difference Vegetation Index (NDVI) value from thermal imagery. However, this was of limited success, as the approach further distorted temperatures in heavily vegetated areas [6].

The methods presented in [6] make a substantial contribution to the study of aerial thermography in archaeology, linking known features to thermal imagery. The comprehensive testing of environmental conditions and material types revealed situations where thermography might excel and others where it might be of lesser use. Furthermore, the successful application of simple quantitative image processing methods indicates the yet untapped potential of thermographic data when using multi-temporal imagery. Expansion of these methods warrants substantial future development.

The most recent investigations of aerial thermography for site prospection take advantage of the next generation of FLIR Vue Pro R sensors. These sensors collect radiometrically corrected data, free from distortions due to the Sun's azimuth, elevation, and atmospheric conditions. Radiometric corrections result in true thermal radiance values and, therefore, greatly improve feature identification on the imagery. Not only are the radiometric images easier to mosaic using popular photogrammetric software, but they also provide substantially increased potential for quantitative image processing by preserving radiance values [7].

These previous studies collectively identify thermal remote sensing as one of the most exciting and innovative advances in archaeological prospection. While the existing research on this topic is both groundbreaking and effective, most of these methods have relied on the analysis of individual thermograms, even when multi-temporal data are available on a site. While analysis of individual thermograms can be productive when the ideal observing conditions are met, the full potential of multi-temporal thermal data remains unexplored. As such, a quantitative image processing method that takes greater advantage of multi-temporal thermal imagery can help overcome these issues and enhance future thermographic efficacy.

III. New Thermographic Quantification for Archeological Site Prospection

Though previous investigations have used thermal remote sensing to detect buried archaeological features, their success has been limited by the data processing methods employed. These investigations have largely relied on visual interpretations of individual thermograms to determine the presence of subsurface anomalies, and as such have produced varied results. Since diurnal cycles affect the radiant temperature of ground materials, these studies rely on ideal data collection windows where the contrast in thermal signatures is most pronounced. Most studies collect multi-temporal thermal imagery at intervals throughout the day. However, their subsequent analysis falls short in exploiting the full potential of these multi-temporal data. In part, this is because non-radiometric thermal data present difficulties when using quantitative image processing methods, as the sensor rescales data in each image, separating the final digital number from collected thermal radiance. In contrast, radiometric thermal data encode calibrated thermal radiance, enabling quantitative image processing methods that greatly increase the potential for thermographic analysis. This allows multi-temporal imagery to be compared using quantitative methods beyond simple visual interpretation.

The proposed thermographic quantification (TQ) prescribes a workflow from data collection and image processing to spatial analysis of a time series of thermograms. TQ requires radiometric thermal sensors, such as a FLIR Vue Pro R models to collect multi-temporal thermal imagery over the course of a day. The first thermal scene should be acquired at dawn, or the earliest flight time possible, with additional imagery collected at successive intervals until dusk, or the latest flight time possible. In addition, a single flight recording reflective spectrum imagery should be conducted at solar noon, when shadow effects are minimized. Like previous investigations, these data are mosaiced, orthorectified, and georeferenced using photogrammetric software such as Agisoft Photoscan Professional. Two variations of an image differencing algorithm are applicable to these multi-temporal thermograms.

First, the thermograms are normalized to a standard range of 0 to 1 so that relative radiant temperature comparisons can be made between images. This is achieved using a simple standard scaling algorithm such as (1):

$$z_i = \frac{x_i - \min(x)}{\max(x) - \min(x)} \tag{1}$$

where x is the original thermogram, x_i is a single pixel, and z_i is the 0 to 1 scaled output pixel value. The scaling algorithm is applied to all images in the time series to produce scaled images in which the minimum and maximum values in the scene are assigned values of 0 and 1, respectively, with all intermediate values assigned floating point values in between.

The effectiveness of this scaling is enhanced by confining the participating pixel values to a targeted area of interest (AOI). Ideally, this AOI should delineate a polygon of relatively homogenous surface characteristics without interfering materials. Undesirable materials might include pronounced above-ground structures or surface materials with outlying thermal response. By confining the range of participating pixel values, the 0 to 1 scaling is distributed only among pixels with consistent surface level characteristics, inducing greater contrast in the scaled thermal output.

From these scaled images, image differencing is used to compare the scaled radiant temperature of each observation relative to the baseline first observation. This is achieved by taking the absolute value of the difference (change in thermal radiance) between the baseline image and each successive observation. These difference images are then averaged, producing a raster of the mean scaled thermal flux relative to the baseline at each location (2):

$$\bar{f}_b = \frac{\sum_{i=2}^{n} | x_i - x_1 |}{n - 1} \tag{2}$$

Where x_i is an individual thermogram observation, x_1 is the baseline first observation, and $\bar{f}_b$ is the mean scaled thermal flux relative to the baseline observation.

Similarly, this image differencing image (IDI) method can be modified to compare images relative to their previous observation, rather than a static baseline (3):

$$\bar{f}_p = \frac{\sum_{i=2}^{n} | x_i - x_{i-1} |}{n - 1} \tag{3}$$

where $\bar{f}_p$ is the mean scaled thermal flux relative to the previous observation.

Since thermal inertia is the property of interest for subsurface prospection, the IDI method compares the relative thermal flux of materials in the scene. With all images set to a standard scale, each resulting difference image will have a uniform value of 0 if changes in radiant temperature are perfectly uniform for all materials. However, as previously discussed, the thermal inertia of each material will cause each to respond to changes in ambient temperature at different rates. Thus, materials that cool or heat more rapidly relative to other materials in the area will have non-zero values in each difference image. Since the magnitude of radiance difference is more important than the direction, the absolute value is taken. Absolute differences also prevent directional shifts (positive and negative) from counteracting each other. The mean scaled thermal flux can then be calculated by summing the individual thermogram differences and dividing by $n - 1$. This mean scaled thermal flux is used to infer the relative thermal inertia of materials in the scene from their radiant temperatures.

If the IDI mean scaled thermal flux is computed within AOIs of uniform surface characteristics, a uniform output would be expected if surface and subsurface conditions are truly homogenous. Of course, this will rarely if ever be the case in practice. Thus, clusters of pixels in the IDI output with distinctly high or low values refer to areas that are changing temperature more rapidly or more slowly, respectively, relative to other materials in the AOI scene. If areas of anomalous mean scaled thermal flux are identified that cannot be correlated with variance in surface reflectance, this enhances the likelihood that the thermal signature is due to subsurface characteristics – or at least that surface reflectance does not adequately explain the thermal anomaly.

Equating variance in thermal flux to subsurface anomalies is bolstered by recognizing areas of varied emissivity. Reflective spectrum imagery can be used to define discrete areas of spectrally similar pixels. Since emissivity is influenced by a material's color, moisture content, surface roughness, etc., spectrally similar pixels are more likely to have similarly uniform emissivity. Due to the high spatial resolution of the reflective spectrum imagery, geographic object-based image analysis (GEOBIA) would be an effective method of segmenting the image. GEOBIA segments an image into image objects by assessing not only individual pixels, but also their surrounding contextual pixels. These methods have been increasingly promoted for use with drone-based imagery, as the increased spatial resolution can induce undesirable noise when per-pixel classification methods are used alone [8]. Segmenting the image into discrete objects can describe areas of uniform reflective characteristics for comparison with the processed thermal imagery.

The above methods describe an image processing workflow with potential to enhance the signature and subsequent detection of subsurface archaeological features. This technique will greatly improve efficacy of thermal anomaly detection by highlighting thermal flux trends through multi-temporal difference imaging. Moreover, thermal features are inferred to be subsurface-induced if they are not readily explained by surface reflectance, mitigating the likelihood of misattributed thermal variance and misidentified subsurface features.

IV. Thermographic Survey at Picuris Pueblo

Fieldwork to collect thermal and reflective spectrum imagery was performed during late June 2018 at Picuris Pueblo, New Mexico. This investigation sought to identify subsurface architectural features surrounding the documented pueblo, covering a survey area of approximately 1.2 hectares.

The environmental conditions of Picuris Pueblo make it an ideal candidate for a case study of the proposed methods. Its high diurnal temperature range during the summer months, with average highs of 26°C and lows dropping to 11°C provide sufficient temperature difference for the relative thermal flux of materials to manifest. Furthermore, the study area has sparse vegetation coverage, which is known to attenuate thermal signatures. Exposed, clay-based soils cover the majority of the site. Thermal differences are enhanced by low average humidity, as dry soils have lower thermal inertia than wet soils and change temperature more readily. Thus, subsurface materials with markedly different thermal inertia from the surrounding soil matrix should induce detectable heating effects on the ground surface.

The data collection strategy employed in this project emphasizes multi-temporal data collection using radiometric thermal sensors and multispectral sensors to collect thermal and reflective imagery over the course of a day. In doing so, a dataset with greater potential for further radiometric processing and quantitative image analysis is achieved. These data were acquired using a FLIR Vue Pro R 640 sensor, GoPro Hero 4 Black sensor, and 3DR Solo sUAS.

In the field, ground control points (GCP) were laid out in a distribution that evenly covered the survey area. These GPS targets were constructed from 60 cm x 60 cm squares of plywood, adorned with a 2 x 2 checkerboard of matte black paint and aluminum foil. The finishes of each section had a dramatic and distinct appearance in the thermal imagery (Fig. 2). Matte black paint has high emissivity, and thus high radiant temperature. In contrast, reflective metal surfaces have a low emissivity. Thus, the foil sections appeared with distinctly low radiant temperature. At 30 cm x 30 cm for each sub-section, the center of the target was easily identifiable in the collected imagery. Geographic coordinates for these targets were surveyed using a Trimble Geo7X GNSS receiver with a Zephyr 2 antenna. Differential corrections were made to these coordinates via continuously operating reference stations (CORS) to achieve a final accuracy of less than 5 cm.

Using the FLIR sensor, thermal infrared data were collected

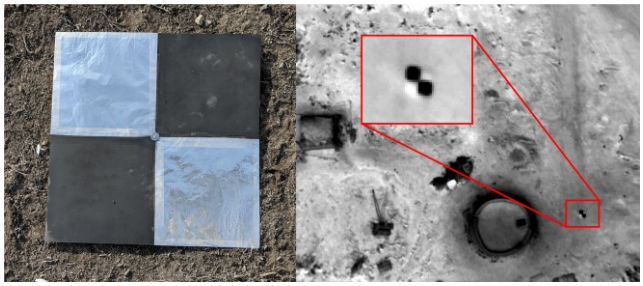

Fig. 2 Ground control point targets, 60 cm x 60 cm square with a 2 x 2 checkerboard of matte black paint and aluminum foil.

from a flight altitude of 70 meters, with forward and side image overlap of 80% flying at 3 meter/second with an anticipated spatial resolution of 6.3 centimeters. While higher resolution imagery could ideally be acquired by lowering the flight altitude, these flight parameters are constrained by the non-adjustable shutter speed of the FLIR sensor and minimum aircraft speed that the drone must maintain [4]. At 1/30th of a second, this relatively long exposure time requires a large ground-sample-distance to avoid excessive pixel blur. Immediately prior to each flight, parameters in the FLIR sensor were adjusted to reflect current environmental conditions, including humidity, ambient temperature, and cloud cover. These adjustments are necessary to collect radiometrically accurate data from the sensor. Thermal imagery was collected in TIFF format with 14-bit radiometric resolution.

To take full advantage of diurnal heat cycles, the first thermal flight was conducted at dawn, approximately 5:30am. This first flight was critical, as it captured thermal imagery at one of the coolest points during the day. If subsurface materials in the scene with a high thermal inertia relative to the surrounding area are present, they might appear as warm objects, retaining their heat through the night. Furthermore, this observation provided a baseline for comparison to following thermal observations, from which IDI processed mean scaled thermal flux was calculated. As such, successive thermal flights were conducted at 9:00am, 1:00pm, 4:30pm, and finally 8:30pm, following the same flight path. Ultimately 5 thermal flights were conducted at 3.5-hour to 4-hour intervals until dusk. Through multiple observations, the diurnal heat flux cycle of materials in the scene could be observed in further analysis and quantitative image processing.

In addition to the FLIR thermal sensor, visible (RGB) spectrum imagery was collected the following day at 1:06pm using the GoPro Hero 4 sensor. This timing corresponded with solar noon at Picuris Pueblo, minimizing the interference from shadows in the reflective spectrum imagery. For the visible spectrum flight, the study area was flow at 35 meters AGL following a cross-grid transect layout at 3 meters/second with 70% side overlap and 80% forward overlap and anticipated spatial resolution of 1.8 centimeters.

These data were processed using Agisoft Photoscan Professional to produce thermal and visible spectrum orthophotos of the study area. In practice the thermal imagery provided a spatial resolution of 6 centimeters, which was standardized across the imagery in final outputs. With the easily identifiable GCP targets and accurate GCP coordinates, these orthophotos were geometrically corrected to achieve an average residual location error of only 0.43 pixels (2.6 centimeters). This high geometric fidelity is critical to image multi-temporal differencing. With an RMSE of less than 0.5 pixels, mathematical operations between successive observations confidently refer to the same ground location. Fig. 3 shows the complete dataset of five thermal orthophotos and the single visible spectrum orthophoto.

V. Analysis and Results

Thermal quantification analysis was performed on two areas of interest across the Picuris Pueblo study area. Using an

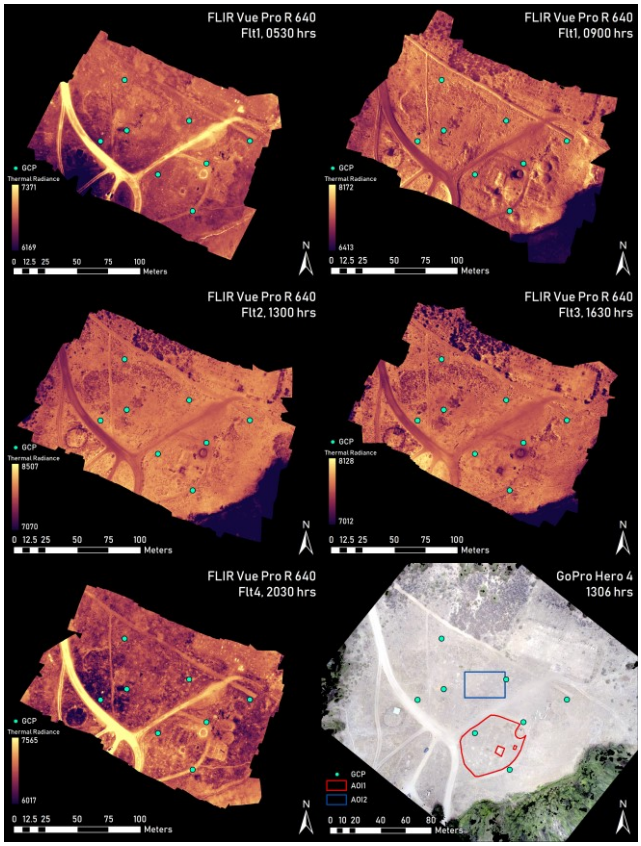

Fig. 3 Five thermal infrared orthophotos, 6 cm spatial resolution, 14-bit radiometric resolution. Single visible spectrum (RGB) orthophoto, 1.8 cm spatial resolution, 8-bit radiometric resolution. Two AOIs are delineated on the visible spectrum orthophoto.

area with previously excavated subsurface features as a training site, the thermal signature of buried structural remains in the unprocessed thermal and IDI mean scaled thermal flux output could be assessed. This signature was then used to classify thermal imagery in a second area of interest with unknown subsurface deposits. This analysis identified multiple thermal anomalies that are likely indicative of subsurface architectural features.

The first area of interest, AOI1, investigated the area immediately surrounding the above-ground roundhouse and kiva, ritual structures presently in use by the Picuris Pueblo community. Documented during early excavations at Picuris Pueblo in the 1960s, multiple phases of architectural features are present in this area [9]. Using the AOI delineation methods described previously, a polygon was draw around these soils of interest, a nearly-homogenous layer of clay-based topsoil, interspersed with upturned soils from rodent bioturbation. Above ground structures such as the roundhouse and kiva were excluded from AOI1, as were GCP targets. This was done so that outlying thermal values would not be included in the range of scaled temperatures, promoting greater contrast in scaled values within the target AOI. All pixels within the AOI1 area were then scaled from 0 to 1, normalizing the range of values from each flight. From these scaled images, the IDI method was applied to enhance the thermal signature of these known subsurface architectural features. IDI comparison to the baseline Flt0 (5:30am) flight and to the previous observation

were performed. Both IDI methods were also run with the Flt1 (9:00am) thermogram removed from the set of observations. This thermogram was characterized by pronounced shadows, introducing undesirable noise in the IDI output.

Of the two IDI methods proposed, differencing relative to the previous observation was more effective than differencing relative to the baseline observation in AOI1. While both methods enhanced the signature of the subsurface walls and room blocks, comparisons to the previous observation were characterized by less noise in the final output. This may be due to suppressed neighborhood effects in IDI processing relative to the previous observation. Features propagate temperature to their surroundings, creating fuzzy boundaries. IDI comparison to temporally adjacent observations suppresses this blooming thermal effect more than comparison to the baseline where the difference is more pronounced. As Fig. 4 indicates, the rectilinear forms of these subsurface features are augmented in the IDI processed imagery. These rough forms closely correlate with site plans from the excavation decades before, indicating that the AREA VI structures of interest have been enhanced through the IDI process.

It should be noted that these IDI images do not represent radiant temperature for any given observation. Rather, they represent relative thermal flux, which is used as an analog for inferring the thermal inertia of materials in the scene. Brighter pixels (high values) indicate a greater rate of thermal flux relative to other materials in the AOI. Conversely, darker pixels indicate lower rate of thermal flux relative to the other materials in the scene. Thus, the rectilinear features in the IDI processed imagery indicate areas with low mean scaled thermal flux relative to the surrounding area. This is expected of subsurface architectural features constructed from clay-rich adobe. The densely packed adobe should resist changes in temperature more than the looser surrounding soil matrix. Subsurface features with sufficiently different thermal fluxes can affect the temperature of surrounding materials. If surface soils are of a homogenous composition and a thermal anomaly in the IDI output transects them, this could indicate that a subsurface feature with a distinct thermal inertia is affecting radiant temperature at the surface. The IDI imagery indicates that the relative thermal radiance of pixels along the rectilinear anomaly is changing less than that of the surrounding area. Thus, it appears that the structural features below contribute an observable difference in thermal radiance trends. Moreover, these features are not plainly visible in any individual thermal orthophoto observation. Rather, they are prominent only when the IDI processing algorithm is applied.

While the thermal imagery enhances the form of these walls, they do also have a visually discernable signature in the reflective spectrum imagery, delineated by soils of a slightly lighter hue than the surrounding area. Nevertheless, GEOBIA segmentation of this visible spectrum imagery is unable to define a corresponding object. Moreover, the confirmed existence of these features based on previous excavations indicates that the IDI process may still be capturing thermal response in the subsurface soil matrix.

AOI2 delineates an area of homogenous soils in the central region of the site. When the scaling and IDI process is applied to AOI2, scaled thermal radiance comparisons relative to the baseline observation appear most effective in this area. Two anomalous clusters of low relative thermal flux are prominent in this IDI output (Fig. 5). The first, Anomaly1, appears as a rectilinear cluster of dark (low thermal flux) pixels in the northwest corner of the AOI. This cluster of pixels measures approximately 8 m x 4 m, consistent with the size of room blocks and structural features in this region. Anomaly2 appears in the east side of AOI2 as a circular cluster of dark pixels, roughly 5 m in diameter. Again, both anomalies appear to have low thermal flux relative to the surrounding materials. Their magnitude of radiant temperature change is on average less

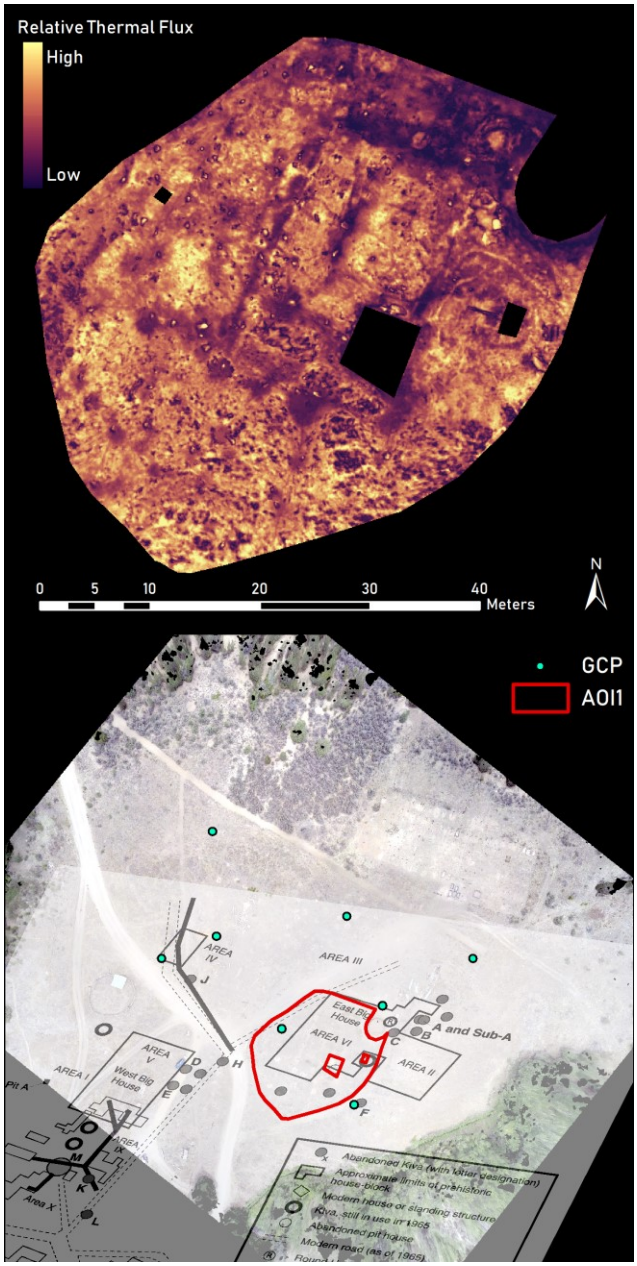

Fig. 4 IDI processed thermal (top) and 1960s-era site plans overlaid on study area (bottom). Rectilinear features are enhanced in the IDI processed thermal imagery, indicating areas of low relative thermal flux. These features correspond with subsurface structural features, as know from previous investigations.

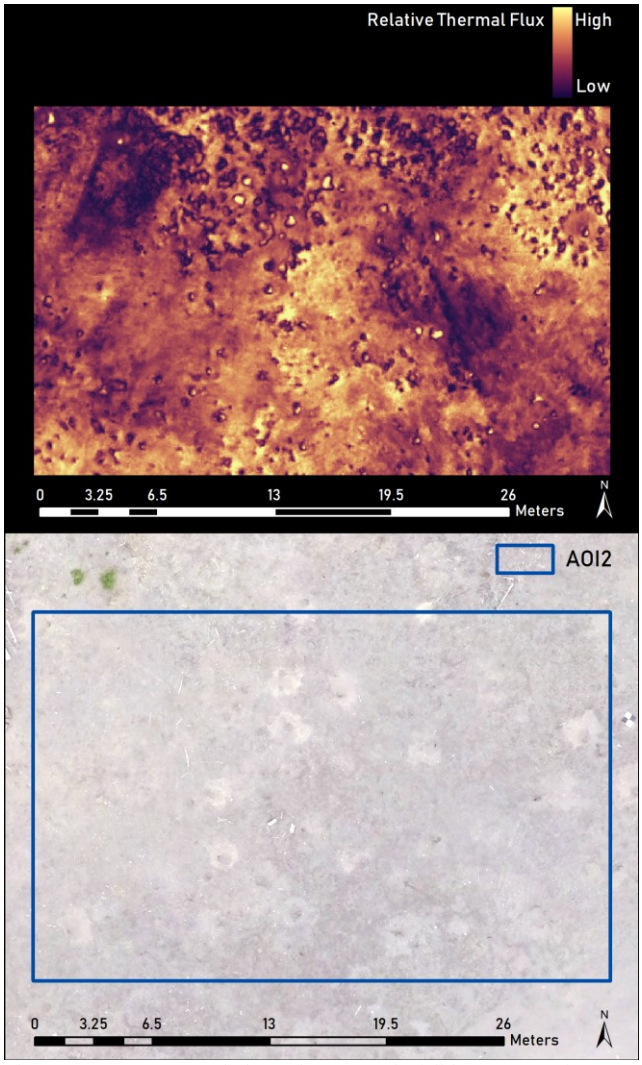

Fig. 5 IDI processed thermal (top) and visible spectrum imagery (bottom). Two thermal anomalies are apparent in the IDI output. These anomalies do not have corresponding variance in the visible spectrum.

than the surrounding area, maintaining a more consistent temperature over the course of the day. Given the size and shape of these features, Anomaly1 may identify the structural remains of another room block like those excavated in AOI1. Anomaly2 may define the extent of a kiva or roundhouse, similar to the above-ground structure on site. These features are most pronounced in the IDI processed raster, with only faint traces in any given thermal observation.

Since AOI1 covers an area with positively identified subsurface features, the signature derived from these rectilinear features is used as training data for supervised classification of additional AOIs. For this, the IDI processed output and unprocessed thermal observations were combined into a six-band raster. Classes corresponding to the locations of rectilinear subsurface features and sterile subsurface areas were selected from this image, creating a vector of radiant temperature trends and IDI derived mean scaled thermal flux from each class. A maximum likelihood classifier was then used to classify each pixel in the according to these classes. As expected, the rectilinear features in AOI1 were captured well, even filtering out some of the dark IDI splotches caused by rodent burrows that might be confused for structural features.

Similarly, the IDI output from AOI2 was stacked with the original thermal orthophotos to produce a six-band raster. The maximum likelihood classifier was used to classify this raster using the same signature file derived from known subsurface features in AOI1. This classification identified the two previously mentioned anomalies as possible subsurface features, along with some additional semi-linear features (Fig. 6). One such feature is located in the north-central area of AOI2 and appears to delineate a three-walled rectilinear form. Similarly, traces of a linear feature are identified in the southwest area of AOI2. The orientation of these extracted features is of significant interest. All rectilinear features appear to follow a southwest-northeast trending orientation – identical to the orientation of features identified in AOI1. This parallel orientation would be expected from accompanying structures in the greater pueblo layout.

What is most exciting is these thermal anomalies and positively classified pixels in AOI2 cannot be correlated with any discernable features in the reflective spectrum imagery. The reflective spectrum imagery appears uniform across this thermal feature's area. There is no indication of soil variance correlated with the thermal feature. This is confirmed through GEOBIA segmentation of the visible spectrum imagery, which segments bioturbated burrows as distinct objects but does not identify any objects corresponding to the thermal features.

Of course, the IDI process and subsequent classification is not without error. There are obvious splotches of noise in the resulting classification, identifying clusters of pixels far too small and dispersed to constitute a subsurface structural feature. Nevertheless, the image processing methodology presented here provides compelling evidence that the larger clusters represent probable subsurface features in an uninvestigated area of the site.

VI. Limitations and Future Goals

This study demonstrates an improved method for subsurface feature prospection through quantitative image processing of thermal imagery. It harnesses spatiotemporal variables extracted from radiometric thermal data to transcend the limitations of pure visual analysis. In doing so ephemeral thermal features are identified in time-series thermal imagery with likely subsurface sources.

Despite the apparent success at locating subsurface features at Picuris Pueblo, further field work will be required to validate these identified features. While the training data were acquired from a location with confirmed subsurface structural features, the features from AOI2 have not been recorded or investigated by any previous research at the site. In the future, ground penetrating radar (GPR) and other geophysical survey methods may be used to corroborate the findings in this study. These methods have decades of proven reliability with success in comparable archaeological landscapes [10]. If these geophysical methods can identify the same anomalies, the veracity of the thermal quantification methods proposed here will be bolstered. Even still, only subsurface excavation can authenticate these features without conjecture.

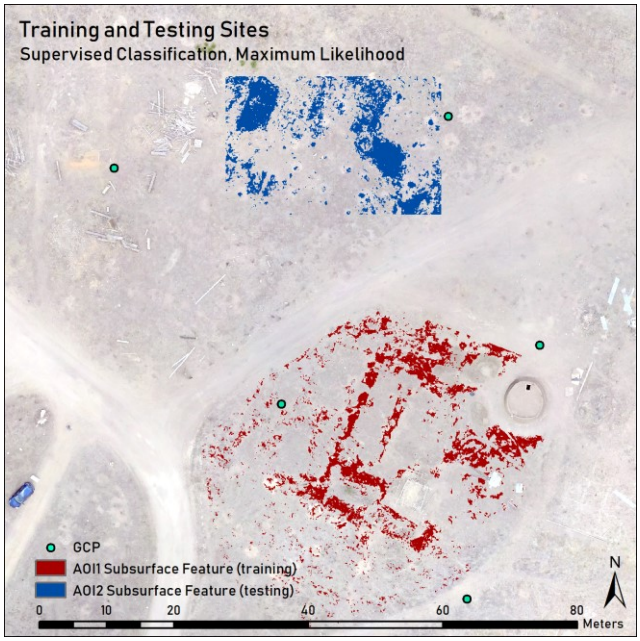

Fig. 6 Classified potential subsurface features from AOI1 (training site) and AOI2 (testing site). Note the parallel orientation of linear features in AOI2 to those in AOI1.

This study underscores the massive potential of thermal remote sensing in archaeological research. The methods presented here are still in their infancy and require considerable development and improvement before the full data potential of radiometric thermal data can be harnessed. Future research towards this goal will focus on applying more sophisticated machine learning models to these data. Using models such as support vector machines, the nuanced relationship between scaled thermal flux and thermal radiance may be better defined, improving the confidence with which prospective features are identified. If reflective spectrum imagery is included in this analysis, greater consideration of surface conditions may be incorporated. This may include automatic delineation of homogenous soil regions, effectively describing AOIs to perform further thermal quantification. Furthermore, thermal features may be compared to the reflective spectrum imagery to check for corresponding features. Thermal features without correlated variance in the reflective spectrum are more likely influenced by subsurface effects, or at least effects beyond the spectral resolution of these non-thermal data.

The imagery processing methods presented in this study explore the dynamic spatiotemporal qualities of thermal imagery. Through a synthesis of time-series observations, the thermal activity at any location over an extended period is expressed. The IDI thermographic quantification process enhances the potential for subsurface features identification by making dynamic thermal properties the quality of interest. This case study at Picuris Pueblo demonstrates the proposed method and its profound advantages over assessments based on the static thermal analysis and visual interpretation alone.

VII. Significance for Picuris Pueblo

Enhanced understanding of the extent and layout of Picuris Pueblo would have substantial cultural and historical significance. One ongoing question shared by many community members is what the village population was prior to, and after, European contact in the 16th and 17th centuries. Very few historical accounts of Picuris population levels exist for this time period, but all agree that Picuris was much larger during this time compared to later occupation levels. If the full spatial extent of earlier, unexcavated structural features can be identified, population estimates for the community may be extrapolated during various occupation phases.

Similarly, aspects of pre- and post-contact period social organization that relate to the size and layout of architectural features, including household organization, size of ritual organizations, and other aspects of past pueblo social structure, can be investigated through architectural remains [11]. An enhanced understanding of site architecture will provide new insights into community social organization through time.

Finally, the potential insights provided by thermal remote sensing provide a non-invasive, non-destructive approach. Much of the archaeological investigations at Picuris Pueblo have relied on excavations and testing that disturbed ancestral parts of this long-lived Native American community [9]. Indigenous communities are increasingly hesitant to undertake disturbance-based investigations of their cultural resources, and thermal imagery provides important insights that can be non-destructive and enhance the preservation of previously unknown buried resources.

References

[1] J. R. Jensen, "Thermal Infrared Remote Sensing," in *Remote Sensing of the Environment: An Earth Resource Perspective*, 2nd ed., Upper Saddle River, NJ: Pearson Prentice Hall, 2006, pp. 249–290.

[2] M. C. Périsset and A. Tabbagh, "Thermal prospection on bare soils," *Archaeometry*, vol. 23, no. 2, pp. 169–187, 1981.

[3] K. Themistocleous, A. Agapiou, B. Cuca, and D. G. Hadjimitsis, "Unmanned aerial systems and spectroscopy for remote sensing applications in archaeology," *Int. Arch. Photogramm. Remote Sens. Spat. Inf. Sci. - ISPRS Arch.*, vol. 40, no. 7W3, pp. 1419–1423, 2015.

[4] J. Casana, J. Kantner, A. Wiewel, and J. Cothren, "Archaeological aerial thermography: A case study at the Chaco-era Blue J community, New Mexico," *J. Archaeol. Sci.*, vol. 45, no. 1, pp. 207–219, 2014.

[5] J. Casana, A. Wiewel, A. Cool, A. C. Hill, K. D. Fisher, and E. J. Laugier, "Archaeological Aerial Thermography in Theory and Practice," *Adv. Archaeol. Pract.*, vol. 5, no. 4, pp. 1–18, 2017.

[6] A. C. Cool, "Aerial Thermography in Archaeological Prospection: Applications & Processing," University of Arkansas, 2015.

[7] H. Thomas, "Some like it hot: The impact of next generation FLIR Systems thermal cameras on archaeological thermography," *Archaeol. Prospect.*, vol. 25, no. 1, pp. 81–87, 2018.

[8] G. Chen, Q. Weng, G. J. Hay, and Y. He, "Geographic object-based image analysis (GEOBIA): emerging trends and future opportunities," *GIScience Remote Sens.*, vol. 55, no. 2, pp. 159–182, Mar. 2018.

[9] M. A. Adler and H. W. Dick, *Picuris Pueblo Through Time: Eight Centuries of Change at a Northern Rio Grande Pueblo*. Dallas, Texas: William P. Clements Center for Southwest Studies Southern Methodist University, 1999.

[10] J. O. Sturm and P. L. Crown, "Micro-Scale Mapping Using Ground-Penetrating Radar" *Adv. Archaeol. Pract.*, vol. 3, no. 02, pp. 124–135, May 2015.

[11] J. Ware, *A Pueblo Social History: Kinship, Sodality and Community in the Northern Southwest.* Santa Fe, New Mexico: School for Advanced Research Press, 2014.